Reactivity of Zirconocene Azametallacyclobutenes: Insertion of Aldehydes, Carbon Monoxide, and Formation of α,β-Unsaturated Imines. Formation and Trapping of [Cp_2Zr=O] in a [4 + 2] Retrocycloaddition[1]

Tracy A. Hanna, Anne M. Baranger, and Robert G. Bergman*

Department of Chemistry, University of California, Berkeley, California 94720

Received December 4, 1995[⊗]

Azametallacyclobutene Cp_2ZrN-*t*-BuCEt=CEt (**1**) underwent an insertion reaction with CO to form the acyl complex **2** (Cp_2Zr(N-*t*-BuCEtCEtCO), 67% yield). The addition of acetone to azametallacyclobutene **3** (Cp_2Zr(NArCMeCPh), Ar = 2,6-dimethylphenyl) yielded the N-bonded enamine and O-bonded enolate complex of zirconocene **4** (Cp_2Zr(NArCMeCPhH)($OCMeCH_2$), 76% yield). The addition of aldehydes RCOH to metallacycle **3** resulted in the insertion of the aldehyde into the Zr−C bond to form complexes Cp_2Zr(NArCMeCPhCRHO) (**8a**) and Cp_2Zr(NArCMeCPhC(*i*-Pr)HO (**9**) in 85% (R = Ph) and 73% yields, respectively. Similarly, treatment of metallacycle **10** (Cp_2Zr-(NArCEtCEt)) with benzaldehyde yielded the insertion product **11** (Cp_2Zr(NArCEtCEtCPhHO)) in 56% isolated yield. The structure of complex **11** was confirmed by an X-ray crystallographic study. Heating the insertion products **8a** and **9** led to elimination of the α,β-unsaturated imines **13** and **14a** (ArN=CMeCPh=CRH) in 53% and 72% yields, respectively, and the formation of oxozirconocene oligomer $(Cp_2ZrO)_n$. The oxozirconocene monomer was trapped by dimethylzirconocene, preventing the formation of oligomer and resulting in the isolation of product **15**. A kinetic study of this retrocycloaddition produced the following activation parameters: $\Delta H^{\ddagger} = 26.5$ kcal/mol, $\Delta S^{\ddagger} = 3.48$ eu. A Hammett σ/ρ study showed that electron-donating groups α to the metallacycle oxygen accelerate the retrocycloaddition ($\rho = -0.8$).

Introduction

Metallacyclobutanes, metallacyclobutenes, and oxametallacyclobutanes have been the focus of intense research because of their role as intermediates in polymerization, epoxidation, and oxygen abstraction reactions.[2−4] There has been much less investigation of the synthesis and reactivity of the analogous nitrogen-containing metallacycles, especially azametallacyclobutenes.[5−10] Our interest in the reactivity of azametallacyclobutenes stems from our desire to utilize the reactive fragment [Cp_2-Zr=NR] to synthesize and functionalize organic molecules. Although the imido functionality is common in organometallic chemistry, there have been few examples of productive transfer of NR to organic systems from imido complexes.[3] We recently reported the synthesis of zirconocene azametallacyclobutenes from the addition of alkynes to the reactive intermediate [Cp_2Zr=NR][11,12] and the catalytic hydroamination of alkynes using Cp_2Zr-$(NHR)_2$ as a catalyst.[13,14] A detailed mechanistic study demonstrated the intermediacy of [Cp_2Zr=NR] and an azametallacyclobutene in the hydroamination process. In this paper we report other transformations that can be carried out with zirconocene azametallacyclobutenes and a comparison of the reactivity of metal−nitrogen bonds and metal−vinylic carbon bonds at the same metal center. In particular, we have observed insertion of aldehydes and carbon monoxide into the Zr−C bond. The aldehyde insertion products react further to form α,β-unsaturated imines and [Cp_2Zr=O] via an unusual retro [4 + 2] reaction, and [Cp_2Zr=O] was trapped by dimethylzirconocene.

Results

Reaction of Metallacycle 1 with Carbon Monoxide. Treatment of the *N*-*tert*-butyl metallacycle **1** with carbon monoxide (640 Torr) at 25 °C led to the formation of the insertion product **2** (eq 1). Complex **2** crystallized

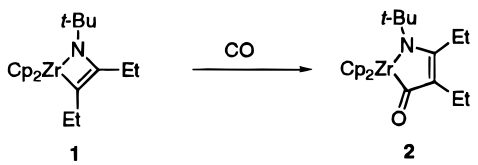

1 2 (1)

⊗ Abstract published in *Advance ACS Abstracts,* June 15, 1996.

(1) Dedicated to Clayton H. Heathcock, a valued colleague and friend, on the occasion of his 60th birthday.

(2) Collman, J. P.; Hegedus, L. S.; Norton, J. R.; Finke, R. G. *Principles and Applications of Organotransition Metal Chemistry*; University Science Books: Mill Valley, CA, 1987.

(3) (a) Wigley, D. E. *Prog. Inorg. Chem.* **1994**, *42*, 239. (b) Nugent, W. A.; Mayer, J. M. *Metal-Ligand Multiple Bonds*; John Wiley & Sons: New York, 1988.

(4) Jørgensen, K. A.; Schiøtt, B. *Chem. Rev.* **1990**, *90*, 1483.

(5) With, J. D.; Horton, A. D. *Organometallics* **1993**, *12*, 1493.

(6) Vaughan, G. A.; Hillhouse, G. L.; Rheingold, A. L. *J. Am. Chem. Soc.* **1990**, *112*, 7994.

(7) (a) A portion of this work has been published in preliminary form: Hanna, T. A.; Baranger, A. M.; Bergman, R. G. *J. Am. Chem. Soc.* **1995**, *117*, 3293. (b) We have also recently synthesized a titanocene azametallacyclobutene from the addition of PhCCH to Cp^*_2Ti=N(*p*-MeC_6H_4). Polse, J. L.; Bergman, R. G.; Andersen, R. A. Unpublished results.

(8) Azametallacyclobutenes have been proposed as intermediates, see refs 9 and 10 and Doxsee, K. M.; Mouser, J. K. M.; Farahi, J. B. *Synlett* **1992**, 13.

(9) McGrane, P. L.; Jensen, M.; Livinghouse, T. *J. Am. Chem. Soc.* **1992**, *114*, 5459.

(10) Wood, C. D.; McLain, S. J.; Schrock, R. R. *J. Am. Chem. Soc.* **1979**, *101*, 3210.

(11) Walsh, P. J.; Hollander, F. J.; Bergman, R. G. *J. Am. Chem. Soc.* **1988**, *110*, 8729.

(12) Walsh, P. J.; Hollander, F. J.; Bergman, R. G. *Organometallics* **1993**, *12*, 3705.

(13) Walsh, P. J.; Baranger, A. M.; Bergman, R. G. *J. Am. Chem. Soc.* **1992**, *114*, 1708 and references therein.

(14) Baranger, A. M.; Walsh, P. J.; Bergman, R. G. *J. Am. Chem. Soc.* **1993**, *115*, 2753.

S0022-3263(95)02156-6 CCC: $12.00

from benzene at 25 °C in 67% yield. A resonance for the acyl carbon was observed at 189.5 ppm in the $^{13}C\{^1H\}$ NMR spectrum (CD_2Cl_2), and the C=O stretch was observed at 1591 cm^{-1} in the IR spectrum (CD_2Cl_2). The data suggest that the acyl group is η^1-bonded to zirconocene as shown in eq 1.[15] When the reaction was performed with ^{13}CO, two quaternary peaks in the $^{13}C\{^1H\}$ NMR spectrum were observed as doublets, one with $^1J_{C-C}$ = 65.3 Hz and the other with $^2J_{C-C}$ = 11.7 Hz. These are indicative of CO insertion into the M−C bond.[16] Although carbon monoxide also reacted with the *N*-aryl metallacycle **3**, the product was insoluble in standard solvents and was not characterized.

Reaction of Metallacycle 3 with Acetone. The addition of acetone to metallacycle **3** after 2 h at 25 °C did not result in the formation of the insertion product but rather in deprotonation of acetone to give the N-bonded enamide/O-bonded enolate zirconocene complex **4** (eq 2). This enolate complex was isolated as orange

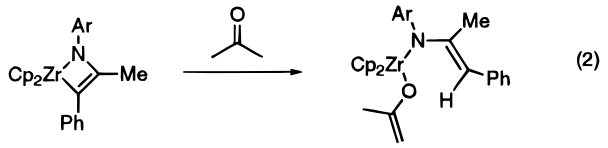

(2)

3 **4**

Ar = 2,6-dimethylphenyl

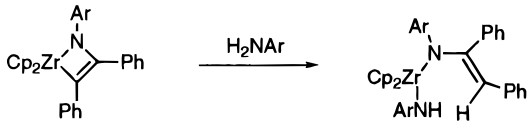

5 **6**

Ar = 2,6-dimethylphenyl

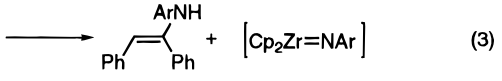

(3)

7

crystals in 76% yield from toluene at −30 °C. Broad lines were observed in the ^1H NMR spectrum at 25 °C, probably due to hindered rotation of the 2,6-dimethylphenyl group. At −50 °C, the vinylic protons of the enolate moiety were observed in the ^1H NMR spectrum at 3.52 and 3.67 ppm (CD_2Cl_2). The vinylic proton of the enamine moiety appeared at 6.32 ppm. These chemical shifts are similar to those observed for other zirconocene enolate complexes.[17−21]

Although its stereochemistry has not been conclusively established, the *E* isomer of the enamide is probably formed as shown in eq 2. We have previously observed the protonation of the diphenyl metallacycle **5** with 2,6-dimethylaniline to form sequentially the enamide amide **6** and then the enamine **7** (eq 3).[13] We determined the geometry of the enamine by X-ray crystallography. It seems likely that protonation with acetone would also result in retention of the geometry of the metallacycle.

Unlike carbon monoxide, the addition of acetone to the *N*-*tert*-butyl metallacycle **1** gave a complex mixture of products over 36 h at 25 °C. The more sterically hindered 2,4-dimethyl-3-pentanone did not react at 25 °C with the *N*-aryl metallacycle **2**; heating at 65 °C for 18 h also gave a multitude of products.

Insertion of Aldehydes into Metallacycle C−Zr Bonds. The addition of benzaldehyde to the dark blue metallacycle **3** in toluene resulted in the formation of the orange complex **8a** over a period of a few minutes at 25 °C (eq 4). Complex **8a** crystallized from a 3:1 mixture of toluene and pentane in 74% yield. We believe the structure of this material is the aldehyde insertion product illustrated in eq 4 based on spectroscopic evidence. Resonances for diastereotopic Cp ligands were

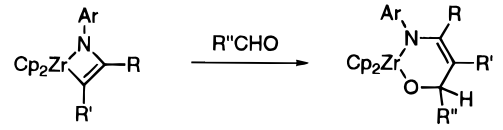

(4)

Ar = 2,6-dimethylphenyl
3 R = Me, R' = Ph
10 R = R' = Et

8a R = Me, R' = R" = Ph
9 R = Me, R' = Ph, R" = *i*-Pr
11 R = R' = Et, R" = Ph

observed in the ^1H NMR spectrum at 5.82 and 6.28 ppm (C_6D_6) and in the $^{13}C\{^1H\}$ NMR spectrum at 111.2 and 113.8 ppm (C_6D_6), indicating the presence of a chiral center. The proton previously bonded to the carbonyl in benzaldehyde exhibited a ^1H NMR chemical shift of 6.22 ppm, significantly upfield from that of free benzaldehyde (C_6D_6, 9.64 ppm). In the $^{13}C\{^1H\}$ NMR spectrum the farthest downfield peak was observed at 155.3 ppm. Since the observed range of chemical shifts for sp^2-hybridized carbons bonded to zirconium is 170−190 ppm,[22−29] the $^{13}C\{^1H\}$ NMR spectrum suggested that no sp^2-hybridized carbons were bonded to zirconium. Therefore, the data are most consistent with the insertion of benzaldehyde into the Zr−C bond.

Similar to benzaldehyde, 2-methylpropionaldehyde reacted over a period of 15 min with metallacycle **3** to give an insertion product (**9**) which was isolated in 73% yield as orange crystals from a mixture of toluene and hexanes at −30 °C (eq 4). The spectroscopic data for insertion product **9** were similar to those of complex **8a**. In the NMR spectrum the diastereotopic Cp resonances for complex **9** were almost (fortuitously) overlapping at 25 °C, but at −40 °C they appeared as resolved singlets at 5.92 and 6.51 ppm in the ^1H NMR spectrum (THF-d_8) and at 111.8 and 114.2 ppm in the $^{13}C\{^1H\}$ NMR spectrum (THF-d_8, −65 °C). The proton previously bonded to the carbonyl in 2-methylpropionaldehyde was

(15) Durfee, L. D.; Rothwell, I. P. *Chem. Rev.* **1988**, *88*, 1059.
(16) Breitmaier, E.; Voelter, W. *Carbon-13 NMR Spectroscopy*, 3rd ed.; VCH: Weinheim, 1987: pp 147.
(17) Veya, P.; Floriani, C.; Chiesi-Villa, A.; Guastini, C. *Organometallics* **1991**, *10*, 2991.
(18) Manriquez, J. M.; McAlister, D. R.; Sanner, R. D.; Bercaw, J. E. *J. Am. Chem. Soc.* **1978**, *100*, 2716.
(19) Moore, E. J.; Straus, D. A.; Armantrout, J.; Santarsiero, B. D.; Grubbs, R. H.; Bercaw, J. E. *J. Am. Chem. Soc.* **1983**, *105*, 2068.
(20) Erker, G.; Dorf, U.; Lecht, R.; Ashby, M. T.; Aulbach, M.; Schlund, R.; Krüger, C.; Mynott, R. *Organometallics* **1989**, *8*, 2037.
(21) Curtis, M. D.; Thanedar, S.; Butler, W. M. *Organometallics* **1984**, *3*, 1855.
(22) Lee, S. Y. Ph. D. Thesis, University of California, Berkeley, 1995.
(23) Buchwald, S. L.; Wannamaker, M. W.; Watson, B. T. *J. Am. Chem. Soc.* **1989**, *111*, 776.
(24) Buchwald, S. L.; Watson, B. T.; Wannamaker, M. W.; Dewan, J. C. *J. Am. Chem. Soc.* **1989**, *111*, 4486.
(25) Schock, L. E.; Brock, C. P.; Marks, T. J. *Organometallics* **1987**, *6*, 232.
(26) Waymouth, R. M.; Santarsiero, B. D.; Coots, R. J.; Bronikowski, M. J.; Grubbs, R. H. *J. Am. Chem. Soc.* **1986**, *108*, 1427.
(27) Thanedar, S.; Farona, M. F. *J. Org. Chem.* **1982**, *235*, 65.
(28) McDade, C.; Bercaw, J. E. *J. Organomet. Chem.* **1985**, *279*, 281.
(29) Jensen, M.; Livinghouse, R. *J. Am. Chem. Soc.* **1989**, *111*, 4495.

Scheme 1

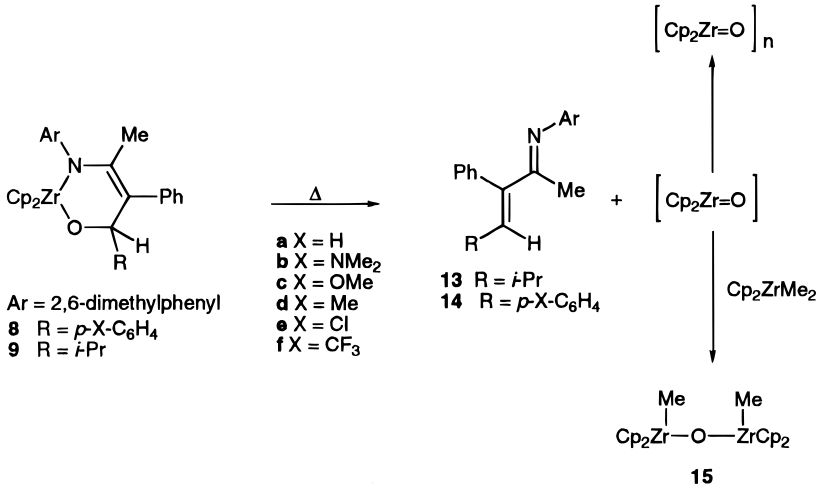

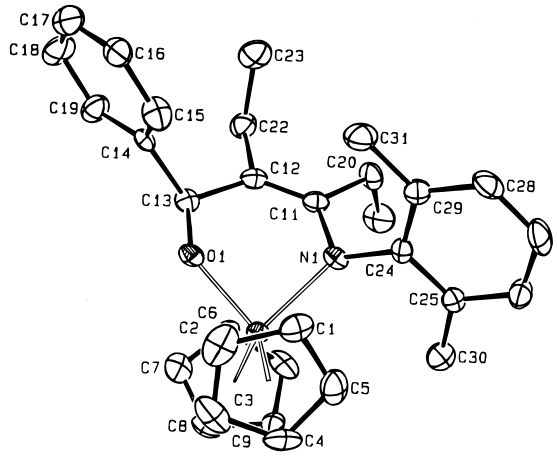

Figure 1. Geometry and labeling scheme for **11**. The ellipsoids are scaled to represent the 50% probabilty surface.

Table 1. Selected Bond Distances and Esd's (Å) for 11

atom 1	atom 2	distance
ZR1	O1	1.969(5)
ZR1	N1	2.110(5)
N1	C11	1.450(8)
N1	C24	1.439(8)
O1	C13	1.399(7)
C11	C12	1.340(9)
C12	C13	1.527(9)

atom 1	atom 2	atom 3	angle
N1	ZR1	O1	87.8(2)
ZR1	N1	C11	115.9(4)
ZR1	N1	C24	127.2(4)
C11	N1	C24	115.8(5)
ZR1	O1	C13	125.6(4)
N1	C11	C12	125.5(6)
N1	C11	C20	113.5(6)
C12	C11	C20	120.8(6)
C11	C12	C13	129.3(6)
C11	C12	C22	119.2(6)
C13	C12	C22	111.5(6)
O1	C13	C12	114.8(6)
O1	C13	C14	108.9(5)
C12	C13	C14	113.2(5)

shown to have a chemical shift in the ^{1}H NMR spectrum of 5.07 ppm. The most deshielded carbon in the ^{13}C{^{1}H} NMR spectrum resonated at 155.7 ppm, consistent with the assignment of complex **9** as a zirconium−carbon insertion product.

Benzaldehyde was found to react analogously with the dark purple metallacycle **10** to yield the orange insertion product **11** at 25 °C in 12 h (eq 4). In addition to inequivalent Cp ligands due to the new stereocenter, the methylene protons in the ethyl groups were observed to be inequivalent by ^{1}H NMR spectroscopy. The proton previously bonded to the carbonyl in benzaldehyde appeared at a chemical shift of 5.85 ppm in the ^{1}H NMR spectrum. The farthest downfield peak in the ^{13}C{^{1}H} NMR spectrum was observed at 155.3 ppm.

Large blocklike orange crystals of **11** were obtained by slow crystallization from 1/1 toluene/pentane over 1 year at −30 °C. The structure of complex **11** was confirmed by an X-ray diffraction analysis of a fragment cut from one of these crystals.[30] An ORTEP drawing is shown in Figure 1, and selected bond distances and bond angles are provided in Table 1. There are two crystallographically independent molecules in the asymmetric unit, related approximately by a translation of 1/2*a*. There are no unusually close contacts between molecules.

(30) The remainder of the crystal was shown to be pure **3** by ^{1}H NMR spectroscopy.

The independent molecules are very similar to each other in configuration. In each case the N−C−C−C−O group is planar to within 0.01 Å, and the $ZrCp_2$ group is substantially out of the plane. The acute angles between the ligand plane and the Zr−O−N plane are 37.5° for molecule 1 and 39.4° for molecule 2. The C═C bond appears to be quite localized. The phenyl ligands are twisted to reduce steric interference, and there is a slight distortion of the Zr coordination from C_{2v} symmetry due to steric interactions.

Metallacycles **3** and **10** did not react with *N*-phenylbenzaldimine or *N*-(2,6-dimethylphenyl)benzaldimine. The *N*-*tert*-butyl-substituted metallacycles **1** and **12** gave complex mixtures of products when heated in benzene in the presence of benzaldehyde or 2-methylpropionaldehyde.

Thermolysis of the Aldehyde Insertion Products To Yield α,β-Unsaturated Imines. Heating the 2-methylpropionaldehyde insertion product **9** for 2 days at 65 °C gave the α,β-unsaturated imine **13** quantitatively by ^{1}H NMR spectroscopy (Scheme 1). The imine was crystallized as white flakes from hexamethyldisiloxane at −30 °C in 53% yield. The IR spectrum contained absorptions at 1629, 1619, and 1593 cm^{-1} (C_6D_6) which are consistent with the C═N stretch of an α,β-unsatur-

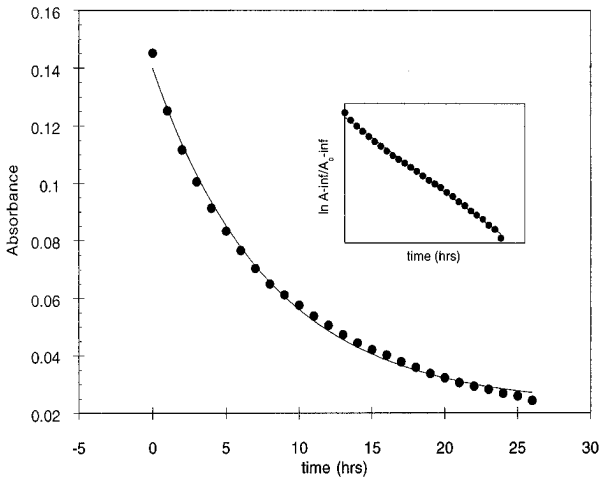

Figure 2. Typical kinetic trace for the retrocycloaddition of **8a** at 45 °C in C_6H_6 followed by UV/vis spectroscopy at 408 nm. The inset shows a plot of ln $(A - A_{inf})/(A_0 - A_{inf})$ vs time for the same data, to illustrate that the kinetics are first order.

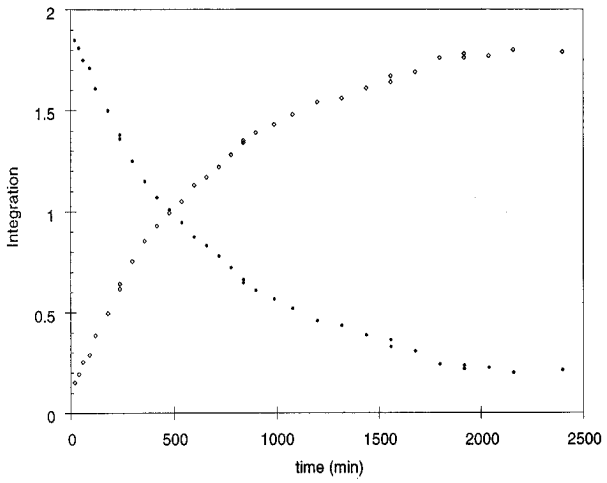

Figure 3. Disappearance of **8a** (solid dots) and appearance of **14a** (diamonds) at 45 °C in C_6D_6 followed by ^{1}H NMR spectroscopy.

ated imine.[31,32] A resonance for the vinylic proton was observed at 6.99 ppm in the ^{1}H NMR spectrum (C_6D_6) and was coupled to the proton on the secondary carbon of the isopropyl group ($^2J_{H-H} = 7$ Hz). Only one of the possible isomeric forms of the imine was observed. The geometry was determined by a NOESY spectrum which showed an NOE cross peak between the methyl group and the vinylic proton. A white precipitate which was not soluble in common organic solvents, believed to be an oligomeric zirconocene oxide (*vide infra*), was formed during the course of the reaction.

The benzaldehyde insertion product **8a** exhibited reactivity similar to that of the 2-methylpropionaldehyde insertion product **9** (Scheme 1). Heating complex **8a** at 45 °C for 3 days resulted in the formation of the α,β-unsaturated imine **14a** and a white precipitate. The imine crystallized from hexamethyldisiloxane at −30 °C in 72% yield. The IR spectrum contained absorptions at 1610 and 1591 cm^{-1} (Nujol). A resonance for the vinylic proton was observed at 7.35 ppm in the ^{1}H NMR spectrum (C_6D_6).

Trapping of [Cp_2Zr=O] Formed in Thermolysis. In previous studies we have found that Cp_2ZrMe_2 is an extremely effective water scavenger, reacting quickly and stoichiometrically with water at room temperature to form the known[33] μ-oxo complex $[Cp_2ZrMe]_2O$ (**15**) and methane. To ensure that the thermolysis of **8a** was occurring under completely anhydrous conditions, we added an excess of Cp_2ZrMe_2 to the zirconacycle **8a** in solution at room temperature. NMR analysis showed the immediate appearance of a small amount (1−3%) of the known[33] μ-oxo complex $[Cp_2ZrMe]_2O$ (**15**) due to scavenging of trace water in solution, but no further reaction with the excess dimethyl complex occurred at 25 °C. The dry solution was then heated to 45 °C to effect conversion of **8a** to the imine. Under these conditions, no white precipitate was formed; instead, a quantitative additional amount (based on **8a**) of $[Cp_2ZrMe]_2O$ (**15**) grew in as the retrocycloaddition reaction proceeded. No other zirconium-containing products were observed (Scheme 1).

Table 2. Rate Constants of Retrocycloaddition 8d + *x* equiv of Cp_2ZrMe_2 → 14d + $[Cp_2ZrMe]_2O$ (15) in C_6H_6 Followed by UV/Vis Spectroscopy at 45 °C

x equiv of Cp_2ZrMe_2	k (s^{-1}) ($\times 10^5$)
0	3.6 ± 0.1
8.4	3.46 ± 0.03
25	3.13 ± 0.03

Table 3. Rate Constants of Retrocycloaddition 8a → 14a + $[Cp_2ZrO]_n$ in C_6H_6 Followed by UV/Vis Spectroscopy

temp (°C)	k (s^{-1}) ($\times 10^5$)
45.0	2.63 ± 0.01
54.6	8.2 ± 0.2
63.6	28.2 ± 0.2
73.6	87.3 ± 0.5

Mechanistic Studies of [4 + 2] Retrocycloaddition. Apparent [4 + 2] retrocycloadditions are relatively rare in organotransition metal ring compounds. Therefore, a kinetic study was carried out to learn more about the mechanism of this reaction. With no dimethylzirconocene present as a trap, the disappearance of starting material was monitored by UV/visible spectroscopy at temperatures between 45 and 75 °C. A representative logarithmic decay and resulting log plot are shown in Figure 2. The reaction was also followed by NMR spectroscopy to confirm that the appearance of imine product exhibited the same rate behavior as the disappearance of starting material. A plot of the disappearance of starting material and appearance of product is given in Figure 3. Measurement of the rate in the presence of both negligible and large amounts of added Cp_2ZrMe_2 had no affect on the measured rate constants (Table 2).

The retrocycloaddition exhibited excellent first-order kinetics at each temperature, yielding the rate constants summarized in Table 3. An Eyring plot of the rate data (Figure 4) gave activation parameters $\Delta H^{\ddagger} = 26.5 \pm 0.7$ kcal/mol and $\Delta S^{\ddagger} = 3.48 \pm 2$ eu.

Electronic effects on the retrocycloaddition were investigated by examining a series of metallacycles (**8a**−**f**) (cf. Figure 5) having different substituents on the phenyl group α to the oxygen atom, prepared by migratory insertion reactions of the appropriate aldehydes. Once again clean first-order kinetics were observed in each

(31) Silverstein, R. M.; Bassler, G. C.; Morrill, T. C. *Spectrometric Identification of Organic Compounds*, 5th ed.; Wiley: New York, 1991.
(32) Pretsch, E.; Seibl, J.; Simon, W.; Clerc, T. *Tables of Spectral Data for Structure Determination of Organic Compounds*; Springer-Verlag: New York, 1983.
(33) Marsella, J. A.; Folting, K.; Huffman, J. C.; Caulton, K. G. *J. Am. Chem. Soc.* **1981**, *103*, 5596.

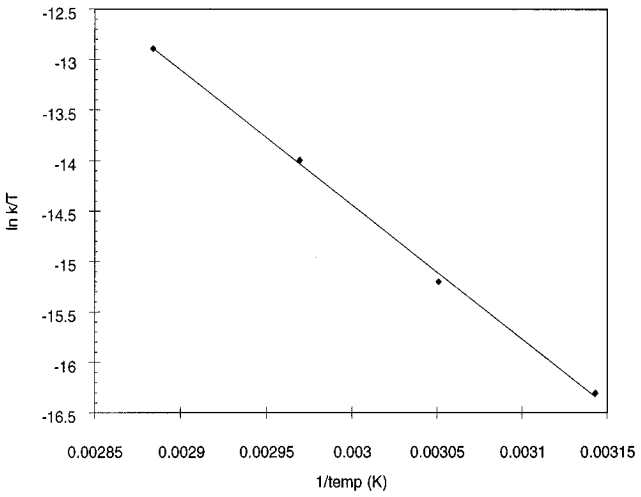

Figure 4. Eyring plot for **8a** → **14a** + $[Cp_2ZrO]_n$ over a temperature range of 45−74 °C.

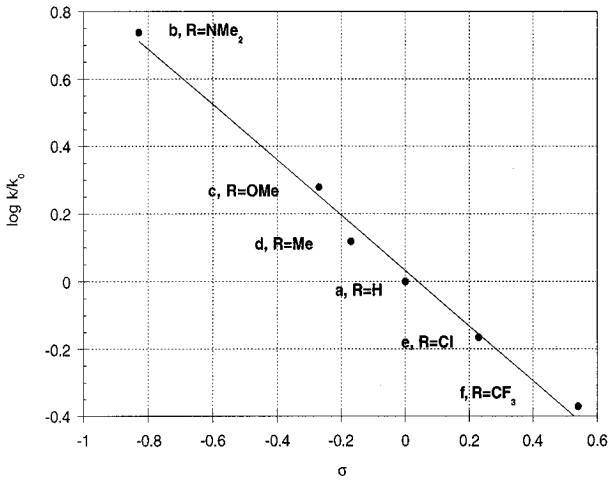

Figure 5. Hammett plot for retrocycloaddition of **8a**−**f** at 45 °C.

Table 4. Rate Constants of Retrocycloaddition 8f + *x* equiv of 14f → 14f + $[Cp_2ZrO]_n$ in C_6H_6 Followed by UV/Vis Spectroscopy

x equiv of **14f**	k (s^{-1}) ($\times 10^4$)
0	3.97 ± 0.03
3.5	3.12 ± 0.08
8	4.7 ± 0.1
10	3.45 ± 0.03

thermolysis. A Hammett plot of the data is shown in Figure 5; the ρ value for the reaction is −0.8.

In order to obtain information about the charge polarization during the reaction, the rate constants in solvents of different polarities were measured. In benzene the first-order rate constant at 74 °C is (8.7 ± 0.5) × 10^{-4} s^{-1}, while in tetrahydrofuran the rate constant is (6.39 ± 0.06) × 10^{-4} s^{-1}. Attempts to measure the rate in more polar solvents such as acetonitrile and DMF were unsuccessful due to reaction with the solvent.

The possibility of a reverse reaction of $Cp_2Zr{=}O$ with an α,β-unsaturated imine was sought by examining the retrocycloaddition of *p*-NMe_2-substituted metallacycle **8b** with an excess of *p*-CF_3-substituted imine **14f** (eq 5). This combination was chosen because complex **8b** undergoes retrocycloaddition readily at room temperature, whereas **8f** is completely stable under these conditions. However, no exchange to give **8f** was observed at room temperature over several days as **8b** decomposed to imine **14b** and $[Cp_2Zr{=}O]_n$. Addition of imine **14f** to the retrocycloaddition of **8f** also had a negligible effect on the rate (Table 4).

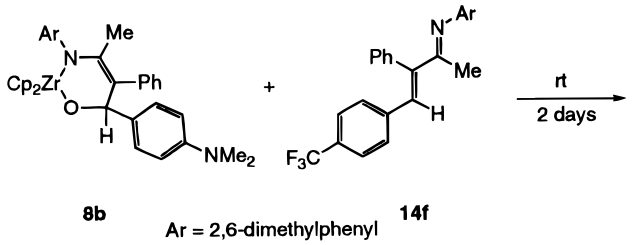

8b **14f**

Ar = 2,6-dimethylphenyl

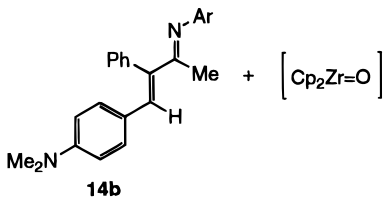

14b

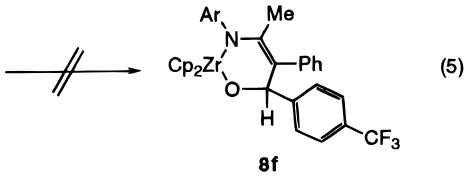

(5)

8f

Discussion

Reaction of Azametallacyclobutenes with CO. Although the *N*-*t*-Bu-substituted metallacycle **1** did not react with aldehydes, we did observe insertion of CO into the Zr−C bond to form the η^1-acyl complex **2** (eq 1). Reaction of CO with Zr−C bonds has been studied extensively and generally leads to η^2-acyl complexes.[15,34] Complex **2** probably exists in an η^1-acyl form due to the ring strain that would result from coordination of oxygen to zirconium.

Reaction of Azametallacyclobutenes with Carbonyl Complexes. The reaction of aldehydes with metallacycles **3** and **10** led to products **8**, **9**, and **11** in which the aldehyde has selectively inserted into the Zr−C bond (eq 4). Buchwald *et al.* observed a similar selectivity for the insertion of aldehydes into the Zr−C bond rather than the Zr−N bond of the zirconocene imine complex **16** (eq 6).[24] In their investigation of the reactivity of the

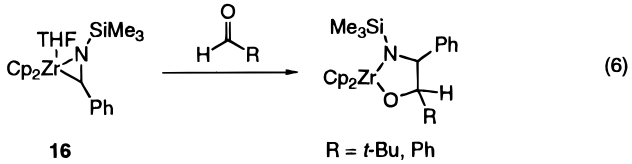

(6)

16 R = *t*-Bu, Ph

oxametallacyclobutene **17**, which is analogous to the azametallacyclobutenes we have prepared,[6] Hillhouse *et al.* found that reactions with aldehydes led exclusively to insertion into the Zr−C bond (eq 7). Doxsee *et al.* have observed insertion of aldehydes and ketones into the vinylic Ti−C bond of titanocene metallacyclobutenes.[35]

(34) Cardin, D. J.; Lappert, M. F.; Raston, C. L. *Chemistry of Organo-Zirconium and -Hafnium Compounds*; Ellis Horwood: New York, 1986.

(35) Doxsee, K. M.; Mouser, J. K. M. *Tetrahedron Lett.* **1991**, *32*, 1687.

For example, addition of acetone to **18** led to insertion product **19** (eq 8). In contrast, we found that acetone undergoes a proton-transfer reaction with **3** to give **4** rather than an insertion product (eq 2).

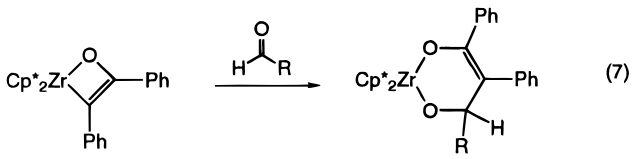

(7)

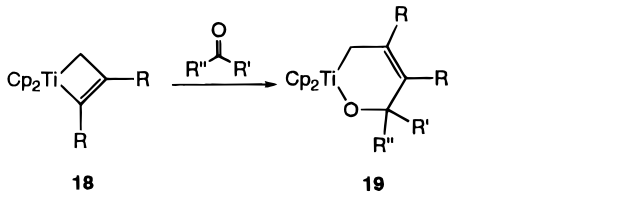

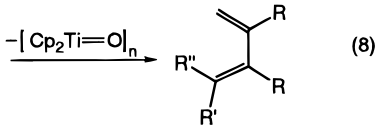

(8)

It is interesting to note that the *N*-*t*-Bu-substituted metallacycles **1** and **12** did not react productively with aldehydes or acetone. This lack of reactivity is probably due to electronic factors rather than steric factors because the substituent on nitrogen is relatively distant from the site of reactivity and *t*-Bu and 2,6-dimethylphenyl groups are not dramatically different in size.

We were interested in the reaction of *N*-(2,6-dimethylphenyl)benzaldimine with **3** because of the possibility of heating the resulting metallacycle and forming the α,*β*-unsaturated imine as is observed with the aldehyde insertion products (eq 9). The zirconocene imido complex

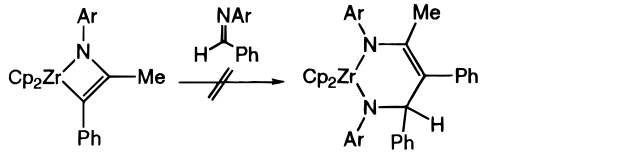

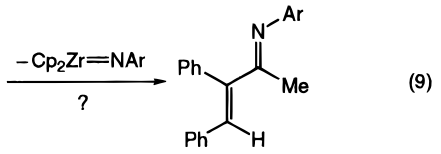

(9)

formed in this reaction could then be trapped with a variety of reagents to support its intermediacy.[11] However, metallacycle **3** was found to be unreactive toward *N*-(2,6-dimethylphenyl)benzaldimine. In addition, *N*-phenylbenzaldimine and 2,4-dimethyl-3-pentanone did not react productively with **3**.

Mechanism of the [4 + 2] Retrocycloaddition. The thermolysis of the aldehyde insertion products **8** and **9** to form α,*β*-unsaturated imines **13** and **14** can be thought of as retro [4 + 2] reactions (Scheme 1). The predominant reactions of M=X complexes with alkenes, alkynes, dienes, and diynes involve overall [2 + 2] additions.[2,3] Overall [4 + 2] additions have been observed in only a few organometallic systems. For example, the reaction of chromium vinylcarbene complexes with alkynes[36] and of titanocene vinylimido complexes with ketones, nitriles, and imines[37] have been proposed to proceed through [4 + 2] mechanisms. Thermolysis of Doxsee's aldehyde and ketone titanocyclobutene insertion products **19** resulted in the formation of 1,3-dienes (eq 8).[35] They proposed both concerted and stepwise reaction pathways for this process. The putative intermediate, [Cp_2Ti=O], was not trapped or characterized.

To investigate the mechanism of the apparent [4 + 2] retrocycloaddition, a kinetic study was undertaken. The activation parameters are similar to those determined for organic retro-Diels−Alder reactions.[38] The small positive activation entropy ($\Delta S^{\ddagger} = 3.48 \pm 2$ eu) is consistent with a unimolecular rate-determining step and may indicate a relatively early transition state. The rate was not affected by the presence of added Cp_2ZrMe_2, demonstrating that the dimethyl complex reacts with an intermediate, most likely [Cp_2Zr=O], generated after the rate-determining step (Scheme 1). The invariance of the rate with excess imine and the lack of exchange of substituted imines into zirconacycle **8b** (eq 5) support a mechanism involving no addition of [Cp_2Zr=O] to **14** to regenerate **8**.

A Hammett study (Figure 5) showed that the reaction is retarded by electron-withdrawing substituents on the phenyl group α to the oxygen atom in zirconacycles **8a**−**f**, giving a ρ value of −0.8. This indicates that there is a buildup of positive charge in the transition state on the carbon α to the oxygen, or alternatively that the starting material **8** is stabilized by electron-withdrawing substituents on the phenyl ring. In order to obtain information about which of these interpretations is more likely, a preliminary investigation of the dependence of the reaction rate on solvent polarity was undertaken. When the retrocycloaddition was repeated in tetrahydrofuran (dielectric constant (ϵ) = 7.58) rather than benzene (ϵ = 2.28), the rate was actually slightly slower. This favors a ground-state stabilization effect. We believe this is due to inductive stabilization of the polarized $Zr^{\delta+}$--$O^{\delta-}$ bond adjacent to the substituted aromatic ring.

Trapping of Oxozirconocene. Group 4 oxometallocene complexes have been found to be very reactive and are often difficult to isolate, but the somewhat less reactive monomeric titanocene and zirconocene intermediates [Cp^*_2Zr=O] and [Cp^*_2Ti=O], containing sterically bulky (η^5-C_5Me_5) ligands, have recently been generated and trapped with various organic molecules.[39−43] Bergman *et al.* formed and trapped [Cp^*_2Zr=O] in the following low-temperature reaction (eq 10) (an earlier high-temperature route was reported by the same group),[40,41,44] and Parkin *et al.* succeeded in fully characterizing a pyridine adduct (**20**) made by the reaction shown in eq 11. Complex **20** reacts smoothly with a

(36) Xu, Y. C.; Challener, C. A.; Dragisich, V.; Brandvold, T. A.; Peterson, G. A.; Wulff, W. D.; Williard, P. G. *J. Am. Chem. Soc.* **1989**, *111*, 7269.

(37) Doxsee, K. M.; Farahi, J. B.; Hope, H. *J. Am. Chem. Soc.* **1991**, *113*, 8889.

(38) Kwart, H.; King, K. *Chem. Rev.* **1968**, *68*, 415.

(39) Howard, W. A.; Parkin, G. *J. Am. Chem. Soc.* **1994**, *116*, 606.

(40) Carney, M. J.; Walsh, P. J.; Hollander, F. J.; Bergman, R. G. *J. Am. Chem. Soc.* **1989**, *111*, 8751.

(41) Benzonitrile was found to undergo a [2 + 2] reaction with Cp^*_2-Zr=O: Carney, M. J.; Walsh, P. J.; Hollander, F. J.; Bergman, R. G. *Organometallics* **1992**, *11*, 761.

(42) Smith, M. R., III; Matsunaga, P. T.; Andersen, R. A. *J. Am. Chem. Soc.* **1993**, *115*, 7049.

(43) Polse, J. L.; Bergman, R. G.; Andersen, R. A. *J. Am. Chem. Soc.* **1995**, *117*, 5393.

(44) Carney, M. J.; Walsh, P. J.; Bergman, R. G. *J. Am. Chem. Soc.* **1990**, *112*, 6426.

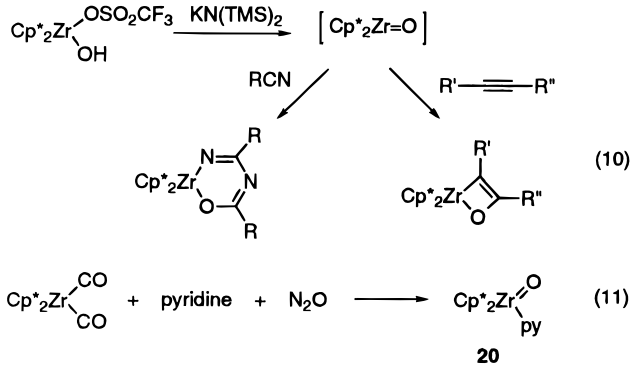

(10)

(11)

number of reagents, in many cases resulting in addition across the Zr=O double bond (eq 12).[39,45]

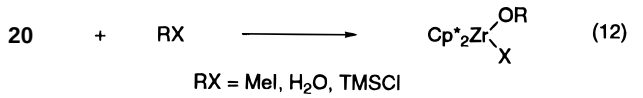

(12)

The titanium analogue was made and trapped in the Andersen and Bergman groups, as shown in eq 13.[42,43] The isoelectronic [Cp_2Zr=NR] has also been shown to react in a [2 + 2] manner (eq 14).[7,22,46,47]

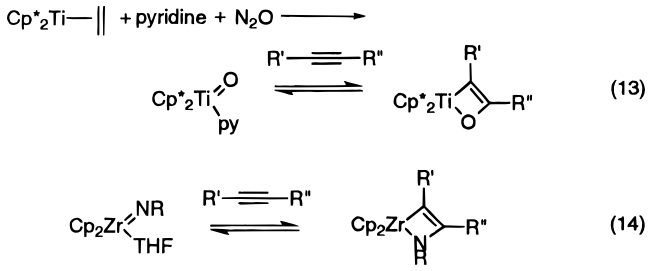

(13)

(14)

The unsubstituted oxozirconacene and oxotitanocene complexes have been postulated as reaction intermediates[22,35,47,48] but have not been unambiguously trapped or characterized. A trimer of [Cp_2ZrO] has been synthesized by two different routes (eq 15),[48,49] while two compounds have been structurally characterized that contain two [Cp_2ZrO] units (eqs 16 and 17).[22,50] It seems possible that the [Cp_2ZrO] fragment—possibly as the free or solvated monomer—is involved in the formation of these compounds.

In the retrocycloaddition described herein (Scheme 1), a concerted reaction mechanism would imply the formation of monomeric [Cp_2Zr=O], which must oligomerize rapidly in a subsequent step. The ability to trap the transient oxozirconocene would strengthen our postulate of its intermediacy and also provide support for the intervention of analogous six-membered oxametallacycle intermediates and their subsequent [4 + 2] retrocycloaddition postulated recently by Doxsee *et al.* (eq 8).[35]

The addition of Cp_2ZrMe_2 resulted in effective trapping of [Cp_2Zr=O], supporting the mechanism illustrated in Scheme 1, in which thermal decomposition of **8** produces

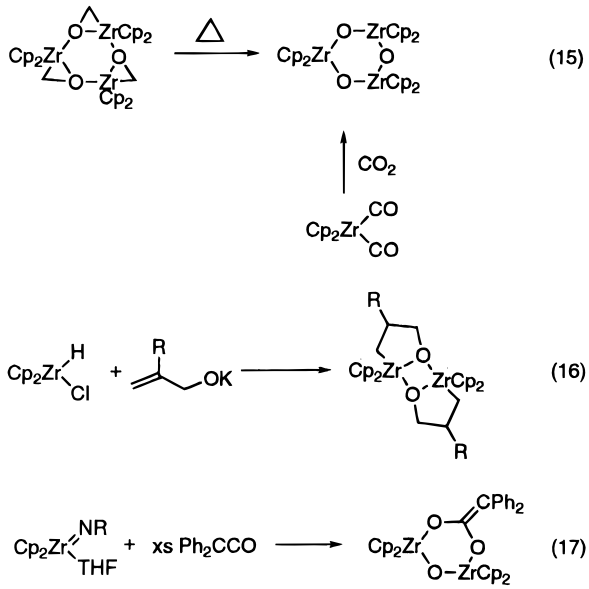

(15)

(16)

(17)

imine **14** and monomeric [Cp_2Zr=O], as would be expected from a simple retrocycloaddition reaction. The oxozirconium complex oligomerizes in the absence of Cp_2ZrMe_2, but in the presence of the dimethyl complex it is efficiently trapped to give the μ-oxo complex **15**.[51]

Conclusion

We have observed the insertion of aldehydes and CO into the Zr−C bond of azametallacyclobutenes. However, the addition of acetone resulted in deprotonation to form an enolate complex rather than insertion. Although the *N*-*tert*-butyl-substituted metallacycle **1** did not react productively with aldehydes and acetone, addition of CO gave the η^1-acyl complex **2**. Thermolysis of the aldehyde insertion products led to an unusual retro [4 + 2] reaction to form α,β-unsaturated imines and [Cp_2Zr=O]. A preliminary investigation of the chemistry of [Cp_2Zr=O] revealed its facile insertion into the Zr−C bond of Cp_2ZrMe_2.

Experimental Section

General. General laboratory procedures have been described elsewhere.[14] Cp_2ZrMe_2,[52] $Cp_2Zr(CH_2CH_2CMe_3)(Cl)$,[53,54] $Cp_2Zr(N(2,6\text{-}Me_2C_6H_3)CMeCPh)$ (**3**),[14] and $Cp_2Zr(NH(2,6\text{-}Me_2C_6H_3))_2$[12] were prepared by literature methods.

$Cp_2Zr(N(t\text{-}Bu)CEt{=}CEt)$ (1). A glass bomb was charged with 3-hexyne (122 mg, 1.49 × 10^{-3} mol), $Cp_2Zr(NH(2,6\text{-}Me_2C_6H_3))_2$ (492 mg, 1.30 × 10^{-3} mol), and 20 mL of benzene. The solution was degassed by 1 freeze−pump−thaw cycle and heated to 75 °C in a constant temperature bath for 2 d, turning dark green after 2 h. The volatile materials were removed under reduced pressure, and the product was crystallized from 2 mL of hexamethyldisiloxane at −30 °C to give green crystals of **1** (411 mg, 1.10 × 10^{-4} mol, 84%): ^{1}H NMR (C_6D_6) δ 0.907 (t, J = 7.36 Hz, 3H), 1.20 (s, 9H), 1.24 (t, J = 7.50 Hz, 3H), 2.44 (q, J = 7.39 Hz, 2H), 2.78 (q, J = 7.51 Hz, 2H), 5.82 (s,

(45) Howard, W. A.; Waters, M.; Parkin, G. *J. Am. Chem. Soc.* **1993**, *115*, 4917.
(46) Lee, S. Y.; Bergman, R. G. *Tetrahedron* **1995**, *51*, 4255.
(47) Lee, S. Y.; Bergman, R. G. *J. Am. Chem. Soc.* **1995**, *117*, 5877.
(48) Fachinetti, G.; Floriani, C.; Chiesi-Villa, A.; Guastini, C. *J. Am. Chem. Soc.* **1979**, *101*, 1767.
(49) Kropp, K.; Stibbe, V.; Erker, G.; Krüger, C. *J. Am. Chem. Soc.* **1983**, *105*, 3353.
(50) Mashima, K.; Yamakawa, M.; Takaya, H. *J. Chem. Soc., Dalton Trans.* **1991**, 2851.

(51) Our identification of the precipitate is based on reaction stoichiometry. To our knowledge, an insoluble oligomeric zirconocene oxide has not been characterized, although the slightly soluble trimeric species [$Cp_2ZrO]_3$ has been previously characterized (see Fachinetti *et al.*, ref 48). A small peak (averaging about 5% of conversion) at δ 6.21 in C_6D_6, corresponding to [$Cp_2ZrO]_3$, is usually observed in our experiments.

(52) Wailes, P. C.; Weigold, H.; Bell, A. P. *J. Organomet. Chem.* **1972**, *34*, 155.
(53) Carr, D. B.; Schwartz, J. *J. Am. Chem. Soc.* **1979**, *101*, 3521.
(54) Hart, D. W.; Schwartz, J. *J. Am. Chem. Soc.* **1974**, *96*, 5115.

10H); $^{13}C\{^1H\}$ NMR δ 12.58, 18.65, 19.26, 28.61, 33.87, 109.52, 120.84, 175.67; HRMS (EI) *m/e* calcd for $C_{20}H_{29}NZr$ 373.1352 (M^+, ^{90}Zr), found 373.1352 (M^+, ^{90}Zr).

Cp_2Zr(N-*t*-BuCEt=CEtCO) (2). A solution of $Cp_2Zr(N(CMe_3)CEt{=}CEt)$ (**1**) (91.3 mg, 2.43×10^{-4} mol) in 7 mL of benzene was degassed by 2 freeze−pump−thaw cycles and placed under 640 Torr of carbon monoxide in a glass bomb. Upon mixing the solution turned from dark green to yellow. After 12 h at 25 °C, approximately 4 mL of the solvent was removed under reduced pressure and a white precipitate formed. The flask was heated at 100 °C until the precipitate redissolved and then was allowed to cool to rt. Small white crystals were obtained (65.7 mg, 1.63×10^{-4} mol, 67%): ^1H NMR (C_6D_6) δ 1.22 (t, J = 7.39 Hz, 3H), 1.31 (t, J = 7.32 Hz, 3H), 1.52 (s, 9H), 2.40 (q, J = 7.43 Hz, 2H), 2.70 (q, J = 7.31 Hz, 2H), 5.83 (s, 10H); $^{13}C\{^1H\}$ NMR (CD_2Cl_2) δ 14.03, 14.67, 24.82, 25.97, 31.82, 54.72, 110.00, 125.45, 170.51, 189.46. Anal. Calcd for $C_{21}H_{29}NOZr$: C, 62.64; H, 7.26; N, 3.48. Found: C, 62.63; H, 6.92; N, 3.43.

Addition of ^{13}CO to Complex 1. An NMR tube was loaded with $Cp_2Zr(N(t\text{-}Bu)CEt{=}CEt)$ (**1**) (20.3 mg, 5.41×10^{-5} mol) and 0.6 mL of C_6D_6. The solution was degassed and placed under 1.5 atm of ^{13}CO. The solution turned yellow and a white precipitate formed. The volatile materials were removed under reduced pressure. The resulting solid was dissolved in 0.6 mL of CD_2Cl_2. The ^1H NMR spectrum showed formation of complex **2**: $^{13}C\{^1H\}$ NMR (CD_2Cl_2) δ 13.99 (s), 14.66 (s), 24.82 (s), 25.97 (s), 31.82 (s), 54.73 (s), 110.03 (s), 125.46 (d, J = 65.29 Hz), 170.55 (d, J = 11.67 Hz), 189.56 (s).

$Cp_2Zr(N(2,6\text{-}Me_2C_6H_3)CPh{=}CMeH)(OC(CH_2)CH_3)$ (4). To a solution of $Cp_2Zr(N(2,6\text{-}Me_2C_6H_3)CMe{=}CPh)$ (**3**) (127 mg, 2.78×10^{-4} mol) in 10 mL of benzene was added acetone (18.0 mg, 3.10×10^{-4} mol). The solution turned from dark blue to yellow in 2 h. The volatile materials were removed under reduced pressure, and the product crystallized from toluene at −30 °C to give orange crystals (109 mg, 2.12×10^{-4} mol, 76%): ^1H NMR (CD_2Cl_2, −50 °C) δ 1.52 (s, 3H), 1.75 (s, 3H), 2.19 (s, 3H), 2.26 (s, 3H), 3.52 (s, 1H), 3.67 (s, 1H), 5.81 (s, 5H), 6.21 (s, 5H), 6.32 (s, 1H), 7.11 (m, 4H), 7.27 (m, 4H); $^{13}C\{^1H\}$ NMR (CD_2Cl_2, −50 °C) δ 15.75, 18.83, 20.52, 23.48, 84.83, 110.64, 112.79, 120.10, 123.62, 120.20, 127.67, 127.96, 128.18, 128.29, 134.20, 136.32, 139.40, 149.88, 154.39, 165.66; HRMS (EI) *m/e* calcd for $C_{30}H_{33}NOZr$ 513.1609 (M^+, ^{90}Zr), found 513.1599 (M^+, ^{90}Zr).

$Cp_2Zr(N(2,6\text{-}Me_2C_6H_3)CMe{=}CPhCH(Ph)O)$ (8a). $Cp_2Zr(N(2,6\text{-}Me_2C_6H_3)CMe{=}CPh)$ (**3**) (276 mg, 6.04×10^{-4} mol) was dissolved in 10 mL of benzene. Upon addition of benzaldehyde in 1 mL of benzene (61.4 μL, 6.05×10^{-4} mol), the color of the solution rapidly changed from dark blue to yellow. The volatile materials were removed under reduced pressure, and the product was crystallized from 3 mL of toluene layered with 1 mL of pentane at −30 °C to give orange crystals (288 mg, 5.12×10^{-4} mol, 85%): ^1H NMR (C_6D_6) δ 1.26 (s, 3H), 2.04 (s, 3H), 2.66 (s, 3H), 5.82 (s, 5H), 6.22 (s, 1H), 6.28 (s, 5H), 7.12 (m, 13H); $^{13}C\{^1H\}$ NMR (C_6D_6) δ 21.17, 21.59, 22.52, 89.90, 111.18, 113.77, 123.68, 126.38, 126.48, 127.29, 127.90, 128.37, 128.58, 128.70, 129.36, 131.02, 133.92, 134.81, 140.54, 144.08, 146.25, 155.03. Anal. Calcd for $C_{34}H_{33}NOZr$: C, 72.55; H, 5.91; N, 2.54. Found: C, 72.58; H, 5.72; N, 2.21.

Complexes **8b**−**f** were prepared by analogous procedures. Spectroscopic and analytical data follow.

$Cp_2Zr(N(2,6\text{-}Me_2C_6H_3)CMe{=}CPhCH(4\text{-}(NMe_2)C_6H_4)O)$ (8b) (57% yield): ^1H NMR (C_6D_6) ($C_6D_5CD_3$) δ 1.28 (s, 3H), 2.03 (s, 3H), 2.49 (s, 6H), 2.76 (s, 3H), 5.84 (s, 5H), 6.21 (s, 1H), 6.28 (s, 5H), 6.56 (d, J = 5.59 Hz, 2H), 7.12 (m, 10H); $^{13}C\{^1H\}$ NMR (−30 °C, $C_6D_5CD_3$) δ 21.5, 21.7, 22.7, 40.3, 89.9, 111.1, 111.7, 113.7, 123.6, 126.3, 128.4, 128.5, 128.6, 129.4, 129.6, 134.0, 134.6, 134.9, 139.7, 144.6, 149.3, 155.2.

$Cp_2Zr(N(2,6\text{-}Me_2C_6H_3)CMe{=}CPhCH(4\text{-}(OMe)C_6H_4)O)$ (8c) (55% yield): ^1H NMR (C_6D_6) δ 1.29 (s, 3H), 2.08 (s, 3H), 2.71 (s, 3H), 3.32 (s, 3H), 5.86 (s, 5H), 6.26 (s, 1H), 6.32 (s, 5H), 6.78 (d, J = 8.7 Hz, 2H), 7.10 (m, 10H); $^{13}C\{^1H\}$ NMR (C_6D_6) δ 20.9, 21.3, 22.2, 54.3, 110.9, 112.5, 113.5, 123.4, 126.1, 127.9, 128.2, 128.4, 128.6, 129.1, 130.8, 133.7, 134.6, 138.4, 140.1, 144.1, 154.9, 158.4. Anal. Calcd for $C_{35}H_{28}NO_2Zr$: C, 71.03; H, 5.79; N, 2.37. Found: C, 70.77; H, 5.86; N, 2.51.

$Cp_2Zr(N(2,6\text{-}Me_2C_6H_3)CMe{=}CPhCH(4\text{-}MeC_6H_4)O)$ (8d) (22% yield): ^1H NMR (C_6D_6) δ 1.25 (s, 3H), 2.03 (s, 3H), 2.09 (s, 3H), 2.68 (s, 3H), 5.81 (s, 5H), 6.22 (s, 1H), 6.26 (s, 5H), 7.12 (m, 12H); $^{13}C\{^1H\}$ NMR (C_6D_6) δ 21.1, 21.2, 21.5, 22.5, 89.8, 111.2, 113.7, 123.7, 126.3, 127.9, 128.1, 128.4, 128.5, 128.6, 129.4, 131.1, 134.0, 134.9, 135.6, 140.5, 143.4, 144.3, 155.1.

$Cp_2Zr(N(2,6\text{-}Me_2C_6H_3)CMe{=}CPhCH(4\text{-}ClC_6H_4)O)$ (8e) (44% yield): ^1H NMR (C_6D_6) δ 1.20 (s, 3H), 1.99 (s, 3H), 2.53 (s, 3H), 5.77 (s, 5H), 6.08 (s, 1H), 6.23 (s, 5H), 7.12 (m, 12H); $^{13}C\{^1H\}$ NMR (C_6D_6) δ 21.1, 21.5, 22.4, 88.9, 111.2, 113.8, 123.8, 126.5, 127.4, 128.1, 128.5, 128.6, 129.2, 129.4, 130.9, 132.1, 133.9, 134.7, 141.0, 143.7, 144.8, 154.9.

$Cp_2Zr(N(2,6\text{-}Me_2C_6H_3)CMe{=}CPhCH(4\text{-}(CF_3)C_6H_4)O)$ (8f) (63% yield): ^1H NMR (C_6D_6) δ 1.23 (s, 3H), 2.03 (s, 3H), 2.55 (s, 3H), 5.84 (s, 5H), 6.15 (s, 1H), 6.28 (s, 5H), 7.12 (m, 10H), 7.36 (d, J = 8.11 Hz, 2H); $^{13}C\{^1H\}$ NMR (C_6D_6) δ 20.9, 21.5, 22.4, 88.9, 111.3, 113.9, 123.9, 124.2 (q, $^3J_{F-C}$ = 3.78 Hz), 126.7, 127.5, 128.1, 128.6, 128.7, 129.4, 130.9, 133.9, 134.6, 141.4, 143.5, 150.3, 154.8 9 (note: CF_3 and C-CF_3 carbons not observed due to low intensity and high coupling to fluorine).

UV Kinetic Studies Using $Cp_2Zr(N(2,6\text{-}Me_2C_6H_3)CMe{=}CPhCH(Ar)O)$ (8). UV/vis spectroscopy was used to study the kinetics of the retrocycloaddition of azoxazirconacyclohexenes **8a**−**f**. Comparison of the UV/vis spectra of **8** and **14** in benzene showed that azoxazirconacyclohexene **8** absorbs in in the visible region (300−500 nm) while imine **14** absorbs only in the UV region. The disappearance of the absorbance due to **8** was therefore followed.

The following stock solutions were prepared in benzene immediately before use: **8a**, 2.0×10^{-4} M; **8b**, 5.3×10^{-4} M; **8c**, 3.7×10^{-4} M; **8d**, 4.4×10^{-4} M; **8e**, 6.7×10^{-4} M; **8f**, 4.8×10^{-4} M. To each solution was added at least 5-fold excess Cp_2ZrMe_2 in order to maintain homogeneity of reactants and products, as well as to scavenge any traces of water present in the solvent. The reaction rate was monitored by following the decrease in absorbance at 406−409 nm due to the disappearance of **8**. The interval between measurements was generally 300 s, but this was increased for slower runs and decreased for faster runs. The reactions were followed for at least 3 half-lives and included at least 20 points.

The procedure used for a typical run follows: A 25 mL volumetric flask was charged with 2.6 mg (4.9×10^{-6} mol) of $Cp_2Zr(N(2,6\text{-}Me_2C_6H_3)CMe{=}CPhCH(Ph)O)$ (**8a**). The solution was then diluted to 10.0 mL using benzene, 10 mg of Cp_2ZrMe_2 (4×10^{-5} mol) was added, and it was mixed by agitating the stoppered flask. A 1.00 cm quartz cell sealed to a Kontes vacuum stopcock was filled with the solution, stoppered in the drybox, and quickly placed in the temperature controller. One room temperature UV/vis measurement was taken. The temperature controller was set to the desired reaction temperature, and when the temperature was reached (indicated by the temperature controller) the kinetic measurements were begun. The sample was allowed to equilibrate for 2 min before measurements were taken, and the first point was discarded in order to insure temperature equilibration. After the reaction had progressed for at least 3 half-lives, measurements were terminated.

The change in absorbance versus time was plotted and the infinity point (A_∞), observed rate constant, and error in the linefit were calculated using a commercial least-squares program (Kaleidograph®) which fit the decreasing exponential to the equation $A = m1 + m2(1 - \exp(-(m3)(m0)))$; where m0 = time, $m1 = A_{inf}$, $m2 = A_0$, and $m3 = k$. Plots of ln $(A - A_{inf})/(A_0 - A_{inf})$ vs time were linear while plots of $1/A$ vs time showed pronounced curvature. A typical plot of absorbance vs time from which the rate constant k was determined is shown in Figure 3. The inset shows a plot of ln $(A - A_{inf})/(A_0 - A_{inf})$ vs time for the same data.

Control experiments verified that the presence of Cp_2ZrMe_2 or excess imine **14** did not affect the measured rate constant. Runs were carried out as described above in the presence of various concentrations of Cp_2ZrMe_2 and imine. The rate constants are listed in Tables 2, 3, and 4.

NMR Kinetic Study Using 8a. An NMR run was carried out at 45 °C to confirm that the growth of products occurred

at the same rate as the disappearance of starting material. $Cp_2Zr(N(2,6\text{-}Me_2C_6H_3)CMe{=}CPhCH(Ph)O)$ (**8a**) (2.7 mg, 5.1 $\times 10^{-6}$ mol) was dissolved in 0.25 mL of C_6D_6, to which was added a solution of 6.5 mg (2.59×10^{-5} mol) of Cp_2ZrMe_2 in 0.25 mL of C_6D_6. The solutions were combined and loaded into an NMR tube attached to a Cajon fitting. The tube was degassed and flame sealed. An initial NMR spectrum was taken; then the NMR tube was placed in an oil bath held at 45 °C (calibrated by thermocouple) for a measured period of time. The tube was removed and cooled, and a one-pulse ^1H NMR spectrum was taken. No reaction occurred while the tube was left at room temperature, as was verified by NMR spectra taken before and after 10 h periods (overnight) at room temperature. The NMR spectra were exponentially multiplied, Fourier transformed, and plotted with integrals. All integral regions had the same limits throughout the series. The data were normalized by holding the sum of the methyl resonances of **8** and **14** constant, and the integrated values of these peaks were plotted against time as shown in Figure 3. The data were analyzed as described above.

From the initial spectrum in the NMR experiment it was determined that 3.2% of the Cp_2ZrMe_2 had initially reacted with water to form $[Cp_2ZrMe]_2O$ (**15**) before the kinetic run was started. In general 0−5% of the Cp_2ZrMe_2 added to retrocycloaddition reactions would react immediately with water, but no further reaction occurred before retrocycloaddition.

$Cp_2Zr(N(2,6\text{-}Me_2C_6H_3)CMe{=}CPhCH(i\text{-}Pr)O)$ (9). A glass bomb was loaded with $Cp_2Zr(N(2,6\text{-}Me_2C_6H_3)CMe{=}CPh)$ (**3**) (262 mg, 5.75×10^{-4} mol) dissolved in 15 mL of benzene. The solution was degassed by 2 freeze−pump−thaw cycles, and isobutyraldehyde was added by vacuum transfer from a known volume bulb (85 Torr, 0.135 L, 6.17×10^{-4} mol). Over a period of 15 min the solution turned from dark blue to orange. After this time, the volatile materials were removed under reduced pressure and the product was crystallized from 5 mL of toluene layered with 2 mL of hexanes at −30 °C to give orange crystals of **9** (223 mg, 4.21×10^{-4} mol, 73%): ^1H NMR (THF-d_8, −40 °C) δ 0.75 (d, J = 6.73 Hz, 3H), 0.83 (d, J = 6.61 Hz, 3H), 1.10 (s, 3H), 1.27 (m, 1H), 2.17 (s, 3H), 2.50 (s, 3H), 5.07 (br, 1H), 5.92 (s, 5H), 6.51 (s, 5H), 6.86 (t, J = 7.38 Hz, 1H), 6.98 (d, J = 6.71 Hz, 1H), 7.03 (d, J = 7.28, 1H), 7.09 (d, J = 7.56, 1H), 7.18 (t, J = 7.29 Hz, 1H), 7.26 (t, J = 7.26 Hz, 1H), 7.36 (t, J = 7.37 Hz, 1H), 7.47 (d, J = 7.70 Hz, 1H); $^{13}C\{^1H\}$ NMR (THF-d_8, −65 °C) δ 17.19, 21.92, 22.25, 22.82, 23.71, 33.99, 91.79, 111.77, 114.17, 123.55, 126.72, 127.12, 128.81, 128.98, 129.15, 129.25, 129.30, 131.07, 134.76, 135.07, 141.84, 145.49, 155.66. Anal. Calcd for $C_{31}H_{35}NOZr$: C,70.40; H, 6.67; N, 2.65. Found: C, 70.25; H, 6.70; N, 2.59.

$Cp_2Zr(N(2,6\text{-}Me_2C_6H_3)CEt{=}CEt)$ (10). A glass bomb was charged with $Cp_2Zr(NH(2,6\text{-}Me_2C_6H_3))_2$ (909 mg, 1.97×10^{-3} mol), 3-hexyne (750 mg, 9.15×10^{-3} mol, 4.6 equiv), and 30 mL of benzene. The reaction vessel was removed to a vacuum line, and the solution was degassed by 1 freeze−pump−thaw cycle and heated to 120 °C for 2 d, during which time it turned from yellow to dark purple. The volatile materials were removed under reduced pressure, and the product was crystallized from pentane at −30 °C to give dark purple crystals (719 mg, 1.70×10^{-3} mol, 86%): ^1H NMR (C_6D_6) δ 0.58 (t, J = 7.45 Hz, 3H), 1.07 (t, J = 7.51 Hz, 3H), 2.11 (q, J = 7.45 Hz, 2H), 2.16 (s, 6H), 2.87 (q, J = 7.51 Hz, 2H), 5.75 (s, 10H), 6.88 (t, J = 7.42 Hz, 1H), 7.10 (d, J = 7.43 Hz, 2H); $^{13}C\{^1H\}$ NMR (C_6D_6) δ 10.98, 17.40, 20.03, 20.69, 28.78, 110.01, 120.31, 121.64, 129.38, 129.44, 150.95, 186.89; MS(EI) m/e 421 [M^+], 41 [base]. Anal. Calcd for $C_{24}H_{29}NZr$: C, 68.19; H, 6.91; N, 3.31. Found: C, 68.00; H, 6.90; N, 3.33.

$Cp_2Zr(N(2,6\text{-}Me_2C_6H_3)CEt{=}CEtCH(Ph)O)$ (11). $Cp_2Zr(N(2,6\text{-}Me_2C_6H_3)CEt{=}CEt)$ (**10**) (290 mg, 6.87×10^{-4} mol) was dissolved in 10 mL of benzene. To this solution was added 79.8 mg (7.53×10^{-4} mol) of benzaldehyde. The solution was stirred for 12 h during which time its color changed from dark purple to orange. The volatile materials were removed under reduced pressure, and the product was crystallized from 1 mL of toluene layered with 0.5 mL of hexanes at −30 °C to give orange crystals of **11** (111 mg, 2.10×10^{-4} mol, 56%): ^1H NMR (C_6D_6) δ 0.851 (t, J = 7.48 Hz, 3H), 0.883 (t, J = 7.39 Hz, 3H), 1.84 (q, J = 7.46 Hz, 2H), 2.04 (m, 2H), 2.13 (s, 3H), 2.50 (s, 3H), 5.67 (s, 5H), 5.85 (s, 1H), 6.15 (s, 5H), 6.94 (dd, J = 8.06 Hz, 6.65 Hz, 1H), 7.03 (d, J = 7.36 Hz, 1H), 7.03 (d, J = 7.36 Hz, 1H), 7.15 (tt, J = 7.35 Hz, J = 1.24 Hz, 1H), 7.29 (t, J = 7.63 Hz, 2H), 7.55 (dd, J = 8.08 Hz, 1.10 Hz, 2H); $^{13}C\{^1H\}$ NMR (C_6D_6) δ 13.91, 13.96, 21.93, 22.15, 25.29, 25.44, 88.43, 111.14, 113.69, 123.32, 125.87, 126.90, 128.06, 129.70, 128.74, 129.31, 133.59, 135.28, 145.78, 147.51, 155.30. Anal. Calcd for $C_{31}H_{35}NOZr$: C, 70.40; H, 6.67; N, 2.65. Found: C, 70.52; H, 6.43; N, 2.76.

Structural Data for 11.[55] Aggregates of large blocklike orange crystals of the compound were obtained by slow crystallization from 1/1 toluene/pentane and washed with pentane. A fragment cut from one of these crystals was mounted on a glass fiber using Paratone N hydrocarbon oil. The crystal was then transferred to our Enraf-Nonius CAD-4 diffractometer and centered in the beam. It was cooled to −109 °C by a nitrogen flow low-temperature apparatus which had been previously calibrated by a thermocouple placed at the sample position. Crystal quality was evaluated via measurement of intensities and inspection of peak scans. Automatic peak search and indexing procedures yielded a monoclinic reduced primitive cell. Inspection of the Niggli values revealed no conventional cell of higher symmetry.

The 7114 raw intensity data were converted to structure factor amplitudes and their esd's by correction for scan speed, background, and Lorentz and polarization effects. No correction for crystal decomposition was necessary. Inspection of the azimuthal scan data showed a variation $I_{min}/I_{max} = 0.94$ for the average curve. An empirical correction based on the observed variation was applied to the data. Inspection of the systematic absences indicated uniquely space group $P2_1/n$. Removal of systematically absent data left 6733 unique data in the final data set.

The structure was solved by Patterson methods and refined via standard least-squares and Fourier techniques. Hydrogen atoms were assigned idealized locations and values of B_{iso} approximately 1.25 times the B_{eqv} of the atoms to which they were attached. They were included in structure factor calculations, but not refined. The final residuals for 613 variables refined against the 3781 data for which $F^2 > 2.5\sigma(F^2)$ were R = 4.15%, wR = 4.24%, and GOF = 1.377. The R value for all 6733 data was 10.1%.

The quantity minimized by the least-squares program was $\sum w(|F_o| - |F_c|)^2$, where w is the weight of a given observation. The p-factor, used to reduce the weight of intense reflections, was set to 0.03 throughout the refinement. The analytical forms of the scattering factor tables for the neutral atoms were used, and all scattering factors were corrected for both the real and imaginary components of anomalous dispersion.

Inspection of the residuals ordered in ranges of sin θ/λ, $|F_o|$, and parity and value of the individual indexes showed a strong variation in agreement factor and intensity comparing reflections with h even to those with h odd. There were no other unusual features or trends. The largest peak in the final difference Fourier map had an electron density of 0.40 $e^-/Å^3$, and the lowest excursion was −0.13 $e^-/Å^3$. There was no indication of secondary extinction in the high-intensity low-angle data.

$(2,6\text{-}Me_2C_6H_3)N{=}CMeCPh{=}CH(i\text{-}Pr)$ (13). $Cp_2Zr(N(2,6\text{-}Me_2C_6H_3)CMe{=}CPhCH(i\text{-}Pr)O)$ (163 mg, 3.09×10^{-4} mol) (**9**) was dissolved in 8 mL of benzene. The orange solution was loaded into a glass bomb, degassed by 1 freeze−pump−thaw cycle, and heated at 65 °C for 2 d. As the reaction progressed the solution turned light yellow and a white precipitate formed. The volatile materials were removed under reduced pressure. The residue was taken up in 5 mL of hexamethyldisiloxane, and the resulting solution was filtered through Celite. The volume of the solution was reduced to 0.5 mL, and snowflake-shaped white crystals were obtained at −30 °C (53.4 mg, 1.83×10^{-4} mol, 53%): ^1H NMR (C_6D_6) δ 0.88 (d, J = 6.27 Hz, 6H),

(55) The author has deposited atomic coordinates for this structure with the Cambridge Crystallographic Data Centre. The coordinates can be obtained, on request, from the Director, Cambridge Crystallographic Data Centre, 12 Union Road, Cambridge, CB2 1EZ, U.K.

1.61 (s, 3H), 1.95 (s, 6H), 2.48 (m, 1H), 6.20 (d, J = 10.1 Hz, 1H), 6.89 (t, J = 7.43 Hz, 1H), 6.99 (d, J = 7.46 Hz, 2H), 7.13 (m, 1H), 7.26 (m, 4H); $^{13}C\{^1H\}$ NMR (C_6D_6) δ 17.00, 18.16, 22.80, 29.04, 122.67, 125.23, 126.96, 128.11, 128.18, 129.90, 139.26, 142.35, 143.33, 150.04, 166.42; HRMS (FAB) m/e calcd for $C_{21}H_{26}N$ 292.2065 ($M^+ + H$), found 292.2064 ($M^+ + H$).

In a separate experiment an ^1H NMR yield was obtained. $Cp_2Zr(N(2,6\text{-}Me_2C_6H_3)CMe{=}CPhCH(i\text{-}Pr)O)$ (21.0 mg, 3.97×10^{-5} mol) and *p*-dimethoxybenzene (4.2 mg, 3.04×10^{-5} mol) were dissolved in 0.8 mL of C_6D_6 and loaded into an NMR tube. The solution was degassed by 2 freeze−pump−thaw cycles, the NMR tube was flame sealed, and two one-pulse ^1H NMR spectra were taken. The sample was then heated at 65 °C for 60 h, and two additional one-pulse ^1H NMR spectra were taken. The yield was determined by integration of the product against the internal standard to be 100% by this method.

(2,6-$Me_2C_6H_3$)N=CMeCPh=C(H)Ph (14a). A bomb was loaded with $Cp_2Zr(N(2,6\text{-}Me_2C_6H_3)CMe{=}CPhCH(Ph)O)$ (**8**) (190 mg, 3.37×10^{-4} mol) and 10 mL of benzene. The solution was degassed and heated to 45 °C for 3 d, during which time it turned yellow and deposited a white precipitate. The volatile materials were removed under reduced pressure, and the residue was taken up in 5 mL of hexamethyldisiloxane. The mixture was filtered, and the filtrate reduced *in vacuo* to 1 mL. Pale yellow crystals of **14a** were obtained at −30 °C (78.5 mg, 2.42×10^{-4} mol, 72%): ^1H NMR (C_6D_6) δ 1.64 (s, 3H), 2.00 (s, 6H), 6.93 (m, 4H), 7.06 (m, 5H), 7.17 (m, 2H), 7.27 (m, 2H), 7.35 (s, 1H); $^{13}C\{^1H\}$ NMR (C_6D_6) δ 17.35, 18.19, 122.84, 125.21, 127.45, 128.10, 128.20, 128.33, 128.80, 130.25, 130.63, 133.61, 136.52, 139.18, 143.58, 150.07, 167.12; HRMS (FAB) m/e calc for $C_{24}H_{24}N$ 326.1909 ($M^+ + H$), found 326.1915 ($M^+ + H$).

Acknowledgment. We are grateful to Dr. F. J. Hollander, director of the University of California, Berkeley, X-ray diffraction facility (CHEXRAY), for performing the crystal structure of complex **11**, to Dr. Robert D. Simpson for assistance with the NOESY spectrum, and to the NIH for financial support through Grant GM-25459.

Supporting Information Available: ^1H NMR spectra for compounds **1**, **4**, **8b**, **8d**, **8e**, **8f**, **13**, and **14a** (9 pages). This material is contained in libraries on microfiche, immediately follows this article in the microfilm version of the journal, and can be ordered from the ACS; see any current masthead page for ordering information.

JO9521561